

Oscillations in Electrochemical Deposition of Zinc

Sheng WANG¹, Ke-Qin ZHANG¹, Qing-Yu XU², Mu WANG^{1,3*}, Ru-Wen PENG¹, Ze ZHANG² and Nai-ben MING¹

¹National Laboratory of Solid State Microstructures and Department of Physics, Nanjing University, Nanjing 210093, China

²Beijing Laboratory of Electron Microscopy, The Center for Condensed Matter Physics and Institute of Physics, Chinese Academy of Sciences, Beijing 100080, China

³International Center for Quantum Structures, Chinese Academy of Sciences, Beijing 100080, China

(Received December 11, 2002)

In this article we report the systematic studies on the oscillation of contrast in front of a growing zinc dendrite in electrochemical deposition observed with interference contrast microscopy. The dependence of the oscillation frequency on the experimental conditions, such as the electric current, the resistance of ion transfer, pH of the electrolyte and the tilting of the electrodeposition cell, etc., has been investigated. The microstructures of the electrodeposits are analyzed with transmission electron microscopy. We conclude that the contrast oscillation in front of the zinc deposit is indeed associated with the concentration oscillation, and is synchronized with the electric voltage/current signals. Although the oscillation can be affected by mass transport in the system, we suggest that it roots from the alternating deposition of zinc and zinc hydroxide on the deposit–electrolyte interface.

KEYWORDS: electrodeposition, oscillation, interfacial kinetics, zinc
DOI: 10.1143/JPSJ.72.1574

1. Introduction

As a typical system to study nonlinear spatiotemporal processes, electro-chemical deposition of metal has been studied for many years.^{1–10} Among many studies, electrodeposition of zinc has attracted much attention since the spontaneous oscillation of electric current/voltage is involved.^{11–15} It has been suggested that unlike many other rhythmicity in electrodeposition,^{16–18} this oscillation is a cathodic process.¹⁵ By carrying out zinc electrodeposition with interference contrast microscopy, we once observed that the contrast in front of the zinc deposit could oscillate,¹⁴ which was ascribed to the oscillation of concentration field of cations during the interfacial growth. Yet the detail analysis showed that the oscillating contrast had a shape of two separated petals,¹⁴ which looked very similar to the banana-shaped contrast distribution induced by the electroconvection.^{19–22} Moreover, the contrast oscillation in front of different deposit branches was very often synchronized, which implied that it might be a collective effect. Therefore it is interesting to identify whether the oscillating contrast observed in the electrodeposition of zinc is truly due to the instability of the concentration field as that suggested in reference,¹⁴ or it is related to the instability of the electroconvection in zinc electrodeposition.

In previous reports of electrodeposition of zinc, the thickness of the electrodeposition cell was usually of the order of sub-millimeter,^{1,2,4,11,15} where both natural convection and electroconvection were unavoidable. In this article, we try to identify the origin of the oscillations in zinc electrodeposition with *in situ* optical observation and *ex situ* microstructural and composition analysis. Associated with the measurement of the responses of the oscillation frequency as a function of experimental conditions, the mechanism of the oscillatory growth in zinc electrodeposition is pinpointed.

2. Experimental Methods and Results

In order to control the thickness of electrolyte layer, we applied a new design to the electrodeposition cell. Unlike the experimental setup reported previously by other groups,^{1,2,4,11,15} where the electrodes were sandwiched between the upper and lower boundaries of the electrodeposition cell, in our experiment the upper glass plate was narrower than the separation of the electrodes. As shown in Fig. 1, four small mica spacers were placed between the upper and lower glass plates. In this way, the thickness of the electrolyte layer is independent of the thickness of the electrodes. Instead, it is controlled by the thickness of the mica spacers, which can be easily adjusted by cleavage. For the experiments reported in this article, the spacer thickness was selected in the range of 80 to 180 μm . Two straight electrodes were fixed on the bottom glass plate in parallel and 10 mm apart. The anode was made of a zinc foil with analytical purity (99.99%), and the cathode was made of a graphite rod. The electrolyte was prepared with 99.9% purity zinc sulfate and deionized water (electrical resistance 18.2 $\text{M}\Omega\cdot\text{cm}$), and the electrolyte concentration was 0.5 M. The electrolyte was filled into the cell by capillary effect. The experiments were carried out in room temperature with potentiostatic or galvanostatic mode (most data were acquired in constant-current mode). The zinc electrodeposition was observed with an optical microscope (Leitz Orthoplan-pol) with transmission interference contrast device and recorded through a video camera system associated with the optical microscope. The cell for electrodeposition was placed on the object stage plate of the microscope. The polarizer and the analyzer of the microscope were adjusted to an almost-perpendicular position in order to achieve the most distinctive interference contrast micrographs. In galvanostatic mode of electrodeposition, the voltage across the anode and cathode or the voltage between the anode/cathode and the reference electrode was collected. Since there existed a pronounced direct-current/voltage background in the measured signal and the alternating signal was weak, an

*To whom corresponds should be addressed.

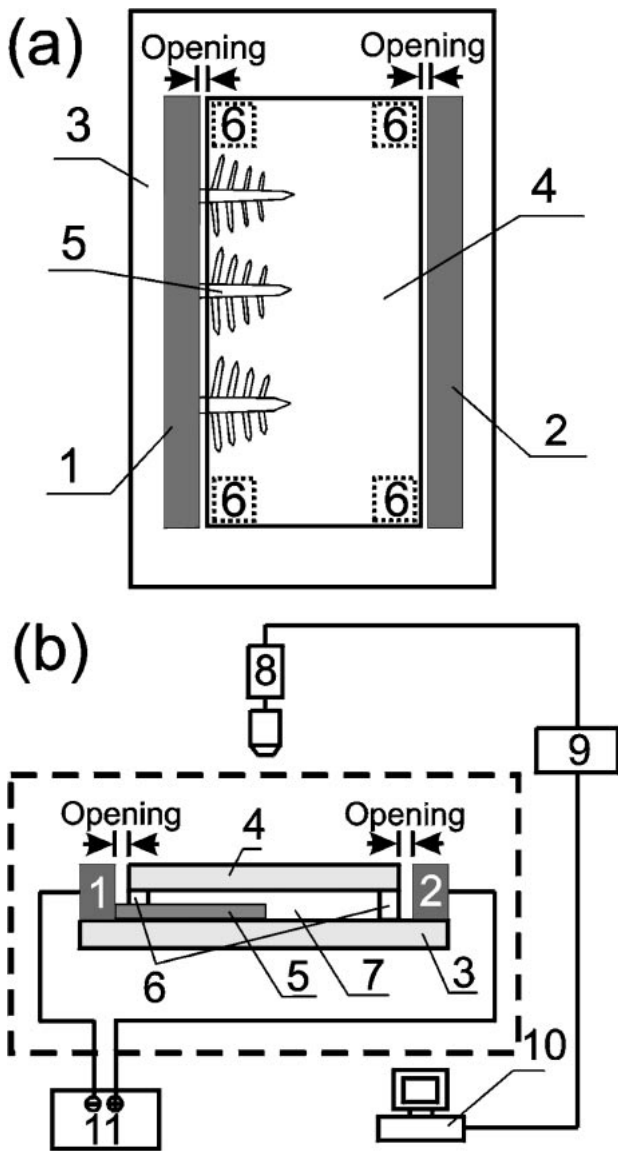


Fig. 1. Schematic diagrams to show the structure of the cell for electrodeposition. (a) top-view of the electrodeposition cell; (b) side-view of the electrodeposition cell. The cell for electrodeposition was placed on the object stage plate of optical microscope for observation. Transmission type of interference contrast microscopy is used to observe the concentration gradient in front of the dendrite tip and to monitor the dendrite growth. To achieve the best contrast of the concentration gradient, the polarizer and the analyzer of the microscopy were adjusted to a nearly perpendicular position. The details of electrodeposition cell: (1) cathode; (2) anode (3) bottom glass plate; (4) top glass plate; (5) dendritic electrodeposits grown from the cathode; (6) mica spacers; (7) electrolyte solution of ZnSO₄ that was filled between the top and the bottom glass plates; (8) CCD video camera; (9) video recorder; (10) computer with 12-bit A/D card for data collection. (11) direct electric power supply.

alternating signal amplifier was used. By using this alternating amplifier, the direct component was filtered, and the enlarged output signal became the differential of the original signal. The amplified signal was then transferred to a computer via a 12-bit A/D card (PCL-818L).

Transmission interference contrast microscopy showed an oscillating contrast distribution around a growing dendrite tip. In interference contrast microscopy the contrast represents the distribution of optical path difference. In our experiments the cell thickness was fixed, and the refractive

index of electrolyte depended on the electrolyte concentration, therefore the contrast actually reflected the electrolyte concentration gradient in the view-field.¹⁴⁾ Figure 2 illustrates the evolution of the contrast in front of a dendrite tip within one period. One may find that the separation between the “petals” varied as a function of time. As illustrated in Fig. 2(a), the separation of the petals was clear, and then it became blurred [Fig. 2(b)]. Finally the separated petals became clear again. This process took place repeatedly and

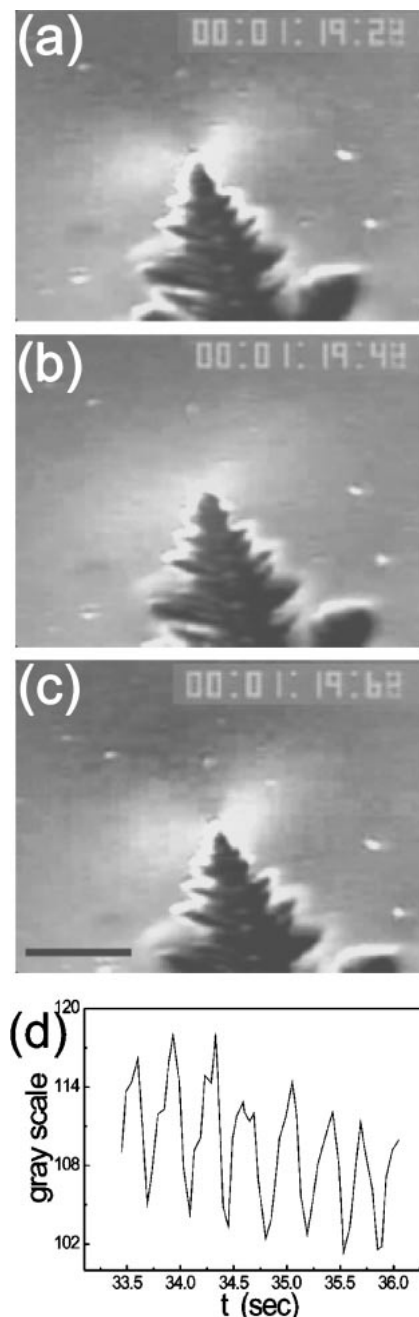


Fig. 2. The successive interference contrast micrographs to show the evolution of contrast in front of a dendrite tip. Two petals can be identified in front of the dendrite tip (a), and the gap between the petals is clear. This gap becomes blurred as the time goes on (b) and eventually it becomes clear again (c). This process continues and forms an oscillation. This time scale is shown at the upper-right corner. The last three digits in the time scale represent minute, second and 1/100 s, respectively. The bar in (c) stands for 20 μm. (d) shows the evolution of the average gray scale in an area (5 μm × 5 μm in size) in front of the tip of a growing dendrite. Oscillation is evident.

generated an oscillation. Typical oscillation period was of the order of 0.4 second. Figure 2(d) showed the evolution of average gray scale in a selected small area in front of the tip ($5\ \mu\text{m} \times 5\ \mu\text{m}$), which quantitatively demonstrates the periodic variation of the local contrast. Since the thickness of the electrolyte film kept constant during electrodeposition, the contrast oscillation was therefore ascribed to the periodic change of the refractive index of the electrolyte, which could be related to the oscillation of the local concentration field. Detail analysis will be given in the section of discussion. Unless especially controlled,¹⁴⁾ the deposit usually consisted of quite a lot of dendrites. We observed that the contrast in front of different dendrite tips oscillated simultaneously when the experiment had been carried out for a few minutes. Corresponding to the contrast oscillation, the electrical voltage/current across the electrodes oscillated simultaneously. Figure 3 shows the oscillation of the voltage across the electrodes (enlarged by the amplifier) as a function of time (when the electrodeposition was carried out in constant current mode) and its fast Fourier transform (FFT), respectively. Periodicity is quite evident.

The anode oscillation in electrochemical systems has been well known.^{16–18)} To identify whether the oscillation observed in our system was anodic oscillation or cathodic oscillation, a reference electrode made of fine platinum filament was used. In the galvanostatic mode we measured the voltage across the cathode and the reference electrode

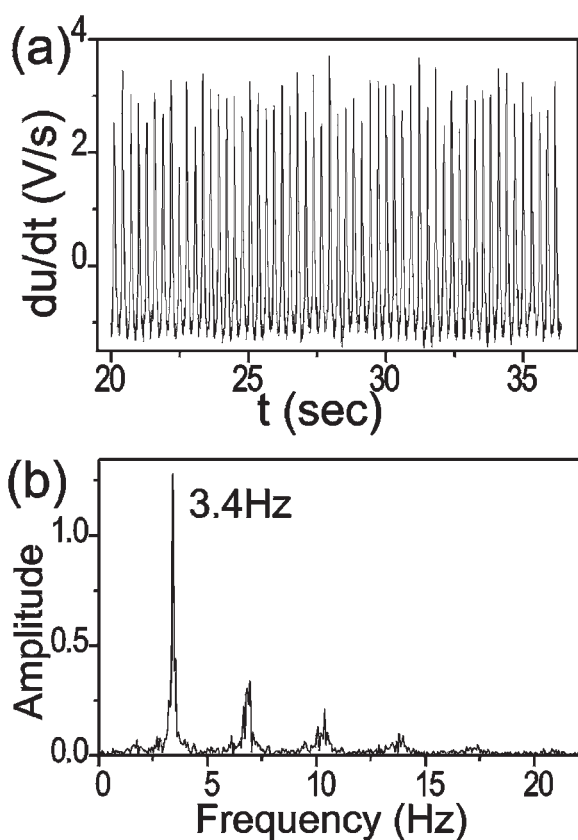


Fig. 3. In the electrodeposition of zinc with galvanostatic mode, oscillation of voltage across the electrodes can be observed. Shown here is the amplified alternating voltage signal (a) and its fast Fourier transform (FFT) spectrum (b). Since an alternating amplifier is used in the experiment, the original signal has been differentiated and enlarged ($\times 300$). For the data shown here the dimension of the electrodeposition cell is $1\ \text{cm} \times 2.5\ \text{cm} \times 80\ \mu\text{m}$. The current is set as 2.0 mA.

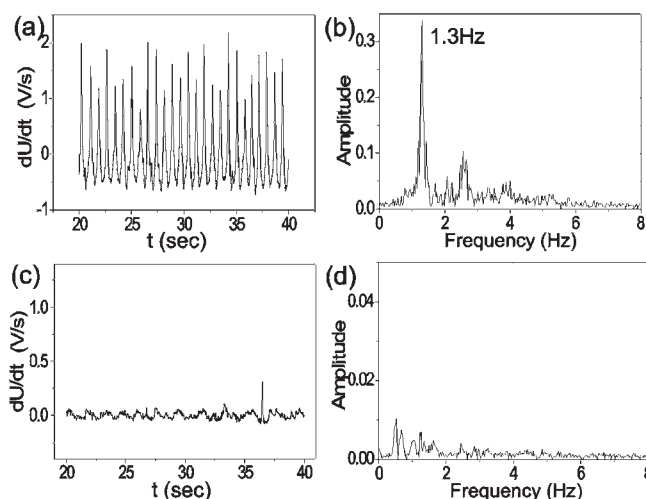


Fig. 4. The plots to show the voltage signals collected across the cathode-reference electrode and anode-reference electrode, respectively. An alternating amplifier ($\times 300$) is used in the data acquisition. (a) The oscillating signal between the cathode and the reference electrode. (b) The FFT spectrum of the data shown in (a). (c) The signal collected across the anode and the reference electrode. (d) The FFT spectrum of the data shown in (c). The dimension of the electrodeposition cell is $1\ \text{cm} \times 2.5\ \text{cm} \times 140\ \mu\text{m}$ for these experiments, and the electric current is set as 2.0 mA.

(via the alternating amplifier). A typical oscillation was observed, as shown in Fig. 4(a). The voltage between the anode and the reference electrode was also measured. As shown in Fig. 4(c), the anode signal was noisy and no regular oscillation could be identified. The difference of the cathode signal and anode signal could be seen more clearly in the FFT spectra. This issue was further checked with *in situ* transmission interference contrast microscopy. When the zinc dendrites developed from the cathode and the oscillation of both contrast and voltage were observed, the poles of the DC power supply were quickly exchanged. In this way previous cathode (zinc dendrites) became the anode, which dissolved gradually. Under the interference contrast microscope the contrast in front of a dissolving dendrite was quite stable [Fig. 5(a)–5(d)]. Figure 5(e) shows the evolution of the average gray scale in a small area ($5\ \mu\text{m} \times 5\ \mu\text{m}$) in front of the dissolving dendrite, no oscillation can be detected.

It should be pointed out that an evident oscillatory growth was usually realized a few minutes after the electrodeposition had been initiated. Similar behavior has been reported by Argoul *et al.*^{15,23)} Before the appearance of regular oscillations, there existed a transitional region where unstable electric voltage/current and the contrast in front of the zinc deposit were observed. In the early stage of electrodeposition FFT of the electric signal showed a broad hump, indicating that quite a lot of frequencies were involved. As the electrodeposition continued, the change of the electric signal became more and more regular. We focused on the regime with regular oscillations. Our measurements indicated that within the first a few minutes the frequency decreased gradually, and finally stabilized, as shown in Fig. 6(a). The oscillation could resume this frequency for about ten minutes when the current was 1.5 mA and the cell thickness was $80\ \mu\text{m}$. In this region, the growth velocity is relatively low (typical value was

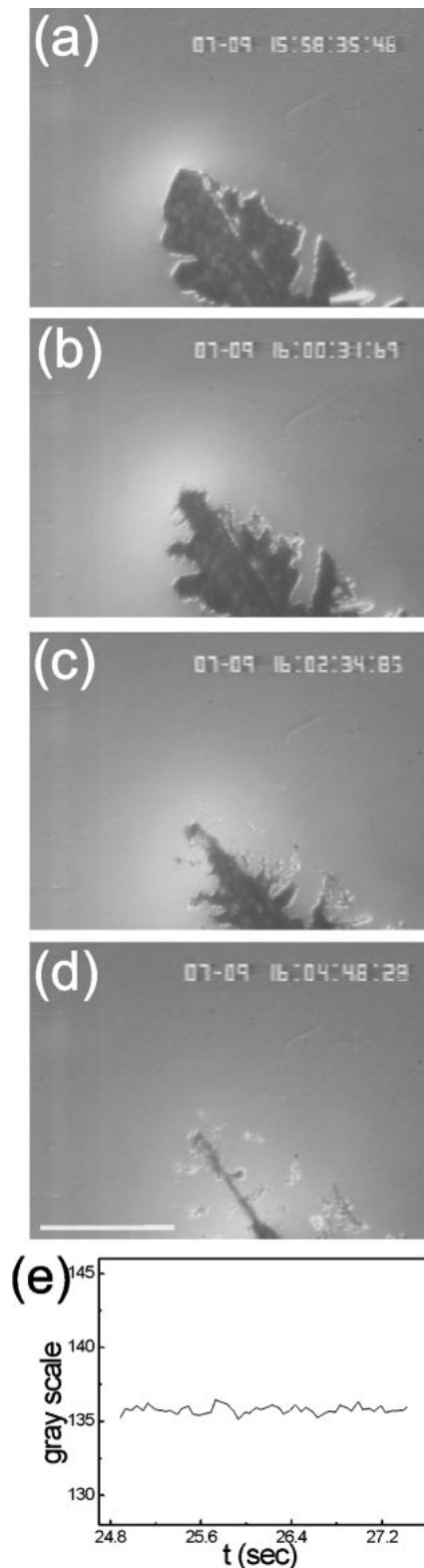


Fig. 5. The interference contrast micrographs to show the evolution of contrast in front of a dissolving dendrite (a–d). The last three digits in the time scale in the upper-right part of the graphs represent minute, second and 1/100 s, respectively. The bar in (d) represents 100 μm . (e) demonstrates the evolution of the average gray scale in an area of $5 \mu\text{m} \times 5 \mu\text{m}$ in front of a dissolving dendrite tip. Comparing to Fig. 2(d) one may find that the contrast shown here is quite stable.

2–6 $\mu\text{m/s}$). As the tips approached the anode, only a few dendritic branches could survive, and the growth velocity became high (typically more than 20 $\mu\text{m/s}$). Meanwhile the concentration field in front of the zinc deposit became

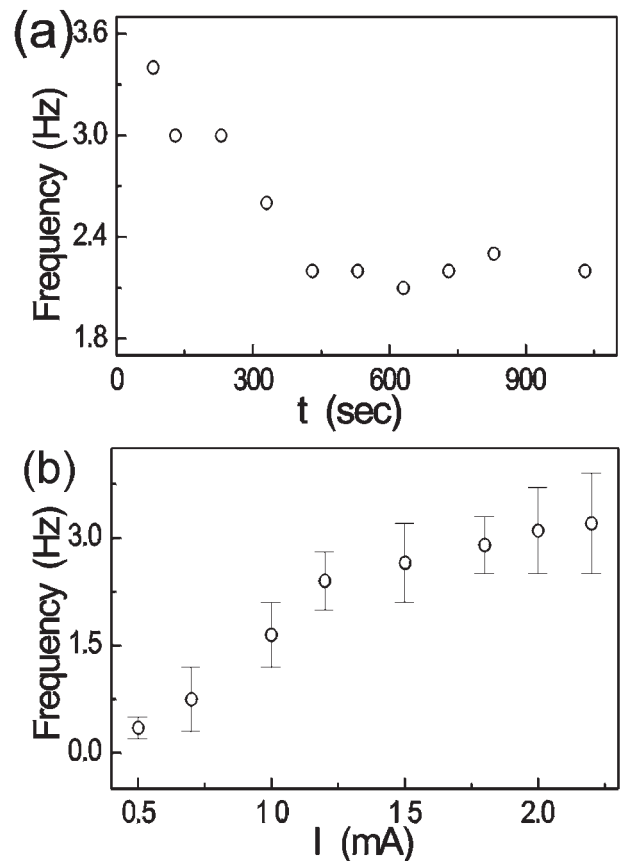


Fig. 6. (a) The evolution of the oscillation frequency in the electrodeposition process. The dimension of the electrodeposition cell is $1 \text{ cm} \times 2.5 \text{ cm} \times 80 \mu\text{m}$ and the current is fixed at 1.5 mA. (b) The oscillation frequency of the voltage across the electrodes measured as a function of the electric current. The data are collected when the regular oscillation has been established.

unstable and the voltage signals were no longer in rhythm.

The dependence of oscillation frequency on the electric current was investigated. As shown in Fig. 6(b), the frequency increased when the electric current became higher. Yet when the current was higher than 1.0 mA, the increase of the frequency was slow down and approached gradually to a constant. If the current exceeded 2.5 mA, the oscillation became unstable. On the other hand, no oscillation could be identified if the applied current was lower than 0.5 mA.

Previously we suggested that the oscillatory behavior in zinc electrodeposition was related to the limitation of mass transport in the system and the nonlinear interfacial kinetics.¹⁴⁾ To verify the role of transportation on the oscillation, we introduced porous material into the system. Standard filter paper was cut into slice with different width, and placed between the anode and the cathode, respectively. We expected that the resistance to the ion transfer increased when the filter paper slice became wider. The observation showed that if the width of the filter paper was below 2 mm, the oscillation was not clearly influenced. Yet as the width of the paper slice was increased, the oscillation frequency decreased gradually, as shown in Fig. 7(a). The influence of the filter paper became even more evident when the dendrite approached the paper slice.

The effect of convection on the oscillation behavior was further studied by control the tilting of the electrodeposition

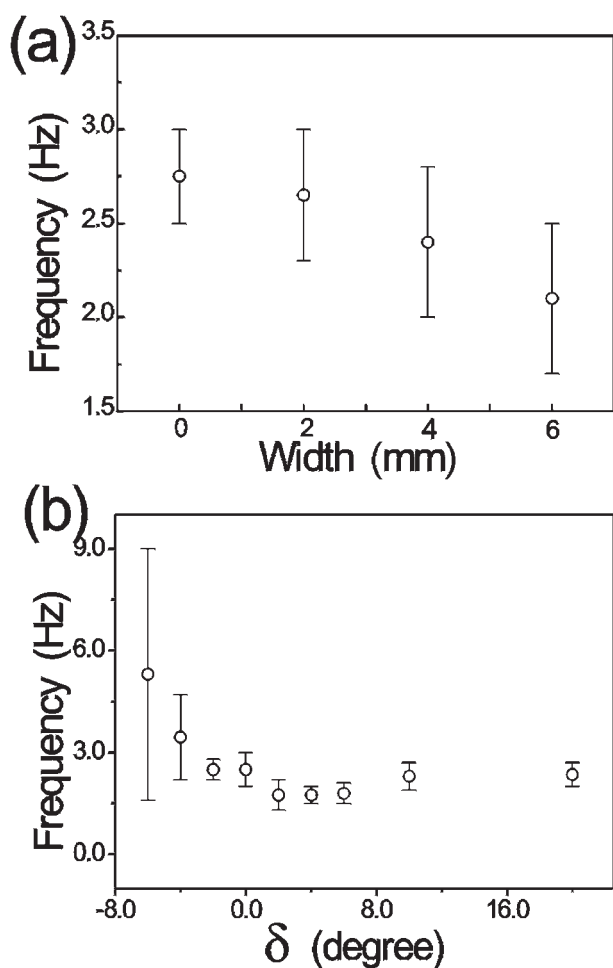


Fig. 7. (a) The oscillation frequency of the voltage across the electrodes measured at different width of the filter paper slice, which is sandwiched between the upper and lower glass plates of the electrodeposition cell. The filter paper slice is arranged in parallel with the electrodes. In these experiments the cell is $1\text{ cm} \times 2.5\text{ cm} \times 180\text{ }\mu\text{m}$ in size and the current is set as 3.5 mA . (b) The oscillation frequency of the voltage signal at different tilting of the electrodeposition cell. δ is defined as the tilting angle of the cell respect to the horizontal plate. For the data shown in (b), the size of the electrodeposition cell is $1\text{ cm} \times 2.5\text{ cm} \times 80\text{ }\mu\text{m}$ and the electric current is 1.5 mA .

cell, which was characterized by δ , the angle of the electrodeposition cell and the horizontal plane. If the cathode was lower than the anode, we defined δ as negative. If the cathode was higher than the anode, δ was defined as positive. In the case of positive δ the tips of the zinc electrodeposits developed with almost the same speed. So the branches of the zinc electrodeposit formed a flat envelop, which was parallel to the electrodes. Meanwhile the oscillation was evident and regular. If, however, the cathode was lower than the anode, i.e., δ was negative, some branches developed faster than the others, and the growth front of the electrodeposits was ragged. Figure 7(b) shows the dependence of the oscillation frequency as a function of δ . It can be found that the oscillation frequency was nearly unchanged when the cathode became higher than the anode up to 20° . When the anode was higher than the cathode, the oscillation frequency increased gradually. When the tilting angle became larger than 5° , the oscillation became unstable: the peaks in FFT of the electric signal were broadened and no isolated peaks could be identified when

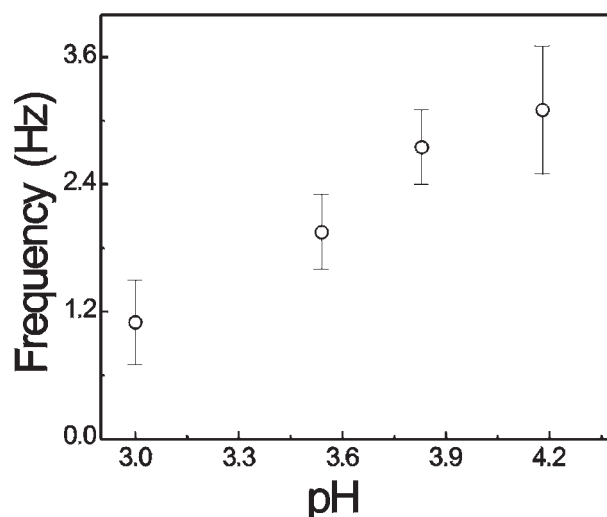


Fig. 8. The oscillation frequency of the voltage across the electrodes measured at different pH of the electrolyte. The dimension of the cell is $1\text{ cm} \times 2.5\text{ cm} \times 80\text{ }\mu\text{m}$ and the electric current is 2.0 mA .

the angle was further increased. These results imply that at least the flow induced by the buoyancy convection is not the origin of the oscillation observed in zinc electrodeposition.

In order to investigate the origin of the oscillatory behavior, we carried out the experiment at different pH of the electrolyte when the other control parameters were unchanged. The pH of the electrolyte was adjusted by adding drops of diluted sulfuric acid to the zinc sulfate electrolyte solution. In our experiments the pH of 0.5 M ZnSO_4 electrolyte was 4.18 without introducing the acid. The lowest pH we achieved was 2.5. We found that by decreasing the pH of ZnSO_4 solution, the oscillation frequency was decreased, as shown in Fig. 8. This effect suggests that the zinc oxide or zinc hydroxide could be responsible for the oscillatory behavior in zinc electrodeposition.

The microstructure of zinc electrodeposit was analyzed with a transmission electron microscope (TEM) (Philips CM200-FEG). Figure 9(a) showed the diffraction contrast image of a zinc dendrite, where the zinc dendrites were faceted. Spatial periodicity could be identified, and it corresponded to the sidebranching of the dendrite. Figure 9(b) showed the electron diffraction pattern of the dendrite, where two phases, zinc and zinc oxide, could be identified. It is known that both zinc and zinc oxide have hexagonal structure. The distinct, bright hexagonally distributed diffraction spots, as that indicated by arrow g_1 , belonged to zinc phase. The adjacent faint diffraction spots, which also possessed a hexagonal distribution, as indicated by g_2 , belonged to zinc oxide. In addition to the spot set of g_2 , there existed three faint polycrystalline rings of zinc oxide. This means that some small crystallites of zinc oxide were randomly orientated [from inner to outer, the rings could be indexed as $(10\bar{1}0)$, (0002) and $(10\bar{1}1)$, respectively]. It should be mentioned that the diffraction pattern shown here was viewed along $[0001]$. From the relation of the diffraction spots of g_1 and g_2 we concluded that the crystallographic orientation of the single-crystalline zinc oxide followed that of the zinc dendrite in electrodeposition. In other words, zinc oxide epitaxially grew on the zinc

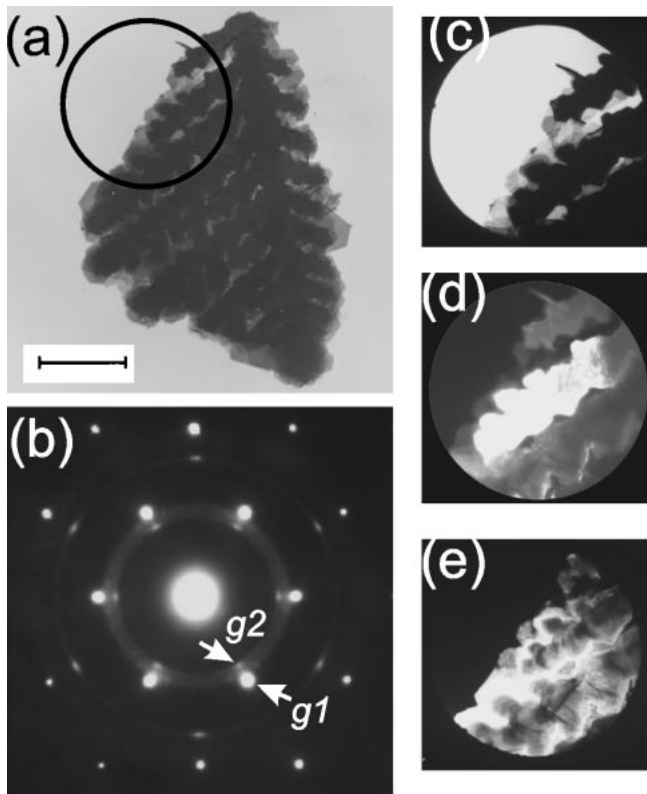


Fig. 9. (a) Electron diffraction contrast micrograph of a zinc dendrite. The bar represents $2\ \mu\text{m}$. (b) The electron diffraction pattern of the dendrite, which is viewed from $[0001]$. The set of the bright diffraction spots indicated by arrow g_1 is generated by zinc. The adjacent faint diffraction spots, as indicated by arrow g_2 , belong to zinc oxide. Both of these two sets of diffraction spots have hexagonal symmetry. In addition to the separated diffraction spots, three faint diffraction rings in between arrows g_1 and g_2 can be identified. From inner to outer side, the ring corresponds to $(10\bar{1}0)$, (0002) and $(10\bar{1}1)$ of ZnO, respectively. (c)–(e) are bright and dark field images of the circled region in (a). (c) shows the bright field image of the dendrite edge. (d) shows the dark field image of zinc, and the diffraction spot g_1 is selected. (e) shows the dark field image of zinc oxide and the diffraction spot g_2 is selected. It can be seen that ZnO exists only around the zinc dendrite.

dendrite. Figures 9(c), 9(d) and 9(e) represented the bright field image and the dark field image of zinc (g_1) and the dark field image of zinc oxide (g_2), respectively, which were taken from the circled region in Fig. 9(a). It can be found that the stem of the dendrite was made of zinc, whereas zinc oxide accumulated around the dendrite. In our experiment immediately after the electrodeposition the electrodeposits were rinsed and dried in nitrogen gas, and preserved in vacuum for further analysis. Therefore it was unlikely that oxidation happened during the sample preparation. Yet it is noteworthy that zinc hydroxide, which could be easily formed when the electrolyte was more basic, might turn into zinc oxide by dehydration. This process could take place when the sample was placed in vacuum. At present stage we are not able to determine exactly whether the zinc oxide was directly generated during the electrodeposition process, or it was transformed from zinc hydroxide.

3. Discussions

In electrodeposition it has been observed that in between the neighboring branches there exists a kind of convection known as electroconvection,^{19–22)} which may affect the

electrodeposition significantly by “driving” the branches to approach each other and forming a network pattern.^{21,22)} The electroconvection is often characterized by a bridge-shaped contrast connecting the neighboring branches of the deposit. We indeed observed that once that the bridge-shaped contrast connecting the neighboring branches fluctuated in electrodeposition. Therefore it is essential to identify whether the oscillating contrast in front of the zinc electrodeposits has any relation with the unstable convection field. Figure 6 indicates that the oscillation may exist when the electric current is as low as 0.5 mA, and the oscillation frequency increases when the current is increased. Yet when the current becomes higher than 1.5 mA the increase rate of the oscillation frequency will be slow down. According to the theory of electroconvection,¹⁹⁾ the strength of the electroconvection is proportional to the strength of the local electric field in front of the deposit branches, which is roughly proportional to the applied electric current/voltage. The nonlinear dependence of the oscillation frequency on the applied current shown in Fig. 6 does not support that the oscillation observed in zinc electrodeposition is related to electroconvection. Another clue comes from the plot of the oscillation frequency as a function of the tilting of the electrodeposition cell. As indicated in Fig. 7, the oscillation frequency does not change very much when the tilting angle varies for more than 20° . Although electroconvection is not directly related to the tilting of the electrodeposition cell (or, the gravity field), yet if the oscillation were convection-related, then we would expect that the oscillation frequency should depend on the tilting of the electrodeposition cell. Therefore, it seems unlikely that the oscillation of the contrast in front of the electrodeposits is associated with the electroconvection.

It is noteworthy that the collective oscillation in the electrodeposition was gradually established. In the early stage of electrodeposition the electric signal was randomly fluctuating. As time went on, perfect oscillation with strict temporal period appeared. According to Figs. 10(e)–10(f), the basic frequency, the second harmonic and the third harmonic frequencies appear almost simultaneously. We suggest that corresponding to the specific experimental conditions there exists a determined basic frequency, which is established via the competition among different oscillations. As a matter of fact, Figs. 10(a)–10(f) show such a spontaneous selection process, where the initial bump with a summit around 10 Hz shifts to low frequency slightly and evolves to several evident discrete peaks. From the dynamic behavior of the contrast in front of each dendrite we can also find that it fluctuates randomly in the beginning, and gradually the contrast fluctuation synchronized to an evident oscillation. We expect that the collective oscillation is a result of the forced resonant process.

It was suggested previously by Suter and Wong that the oscillation of electric signal in electrodeposition was due to the repeated charge accumulation and dielectric breakdown in the double layer on the electrode–electrolyte interface.¹¹⁾ We observed that corresponding to the oscillation of the electric signal, the contrast in front of the growing dendrite oscillated synchronally, which was interpreted as the joint contribution of impurity adsorption and anisotropy on the growing interface.¹⁴⁾ It is generally accepted that impurity is

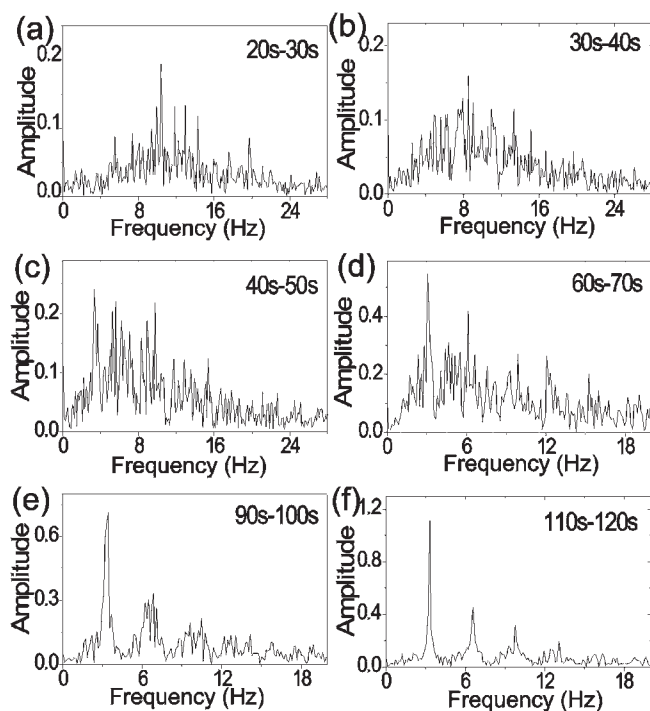
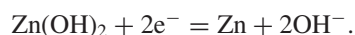


Fig. 10. The FFT spectra of the voltage signal between the anode and the cathode to show the establishing process of a stable oscillation in zinc electrodeposition. The time during which the data are collected is: (a) 20 s to 30 s, (b) 30 s to 40 s, (c) 40 s to 50 s, (d) 60 s to 70 s, (e) 90 s to 100 s, (f) 110 s to 120 s, respectively (the timing starts from the beginning of the electrodeposition). It can be seen that during the establishment of a stable oscillation, the maximum of the bump in FFT shifts slight to the lower frequency (a–b), and then the bump gradually decomposes into several separated peaks. After about two minutes a stable oscillation is established. For these measurements the dimension of the electrodeposition cell is $1\text{ cm} \times 2.5\text{ cm} \times 80\text{ }\mu\text{m}$ and the electric current is 1.5 mA.

required at the growing interface in order to induce an oscillation. Clearly proton reduction is involved in the electrodeposition of zinc from the aqueous solution of ZnSO_4 , and the reduction of zinc and proton is diffusion-limited. The standard equilibrium electrode potentials of zinc and proton are -0.7628 and 0 , respectively. This means that the solution in front of the electrodeposit becomes more basic when the electrodeposition has been carried out for a while. Once this situation occurs, as suggested by Argoul and Kuhn,¹⁵ $\text{Zn}(\text{OH})_2$ will be precipitated on the growing interface and the cation reduction will be prohibited by cathode passivation. As the result, the current is decreased. In galvanostatic mode, in order to resume the present constant current, the power supply will increase the voltage applied across the electrodes. Once this occurs, $\text{Zn}(\text{OH})_2$ will transfer to zinc via the following reaction (the standard electrode potential for the reaction equals to -1.245 V)



In this way the hydroxide layer dissolves entirely, the electrodeposition of zinc is reactivated, and the voltage drops to its initial value. Our observations of TEM support this picture. As indicated in Fig. 9, ZnO exists only on the outer crust of the zinc dendrite, and no ZnO or $\text{Zn}(\text{OH})_2$ has been detected inside the zinc dendrite. It is known that the zinc hydroxide can be dehydrated to ZnO . When we prepare the TEM sample and observe the sample in TEM, the

ultrahigh vacuum environment will rapidly drive water out from the zinc hydroxide. In more acidic solution, it takes longer time to accumulate sufficient amount of $\text{Zn}(\text{OH})_2$ on the growing interface to prohibit the zinc deposition. For this reason, the frequency of oscillation will be lower. This is indeed in agreement with the experimental observations shown in Fig. 8.

4. Conclusion

The oscillation of the contrast in front of a growing zinc dendrite in interference contrast microscopy has been systematically studied. The dependence of the oscillation frequency on the experimental conditions, such as the electric current, the resistance of ion transfer, pH of the electrolyte and the tilting of the electrodeposition cell, etc., has been investigated. We conclude that the contrast oscillation in front of the zinc deposit is associated with the local concentration oscillation, and is synchronized with the electric voltage/current signals. Although the oscillation can be affected by the mass transport in the system, it most likely roots from the alternating deposition of zinc and zinc hydroxide on the deposit–electrolyte interface.

Acknowledgements

This work was supported by the grants from the Ministry of Science and Technology of China (No. G1998061410) and the National Science Foundation of China (No. 19974014 and No. 10021001). Authors would also like to thank Wei Wang and Vincent Fleury for discussions.

- 1) M. Matsushita, M. Sano, Y. Hayakawa, H. Honjo and Y. Sawada: *Phys. Rev. Lett.* **53** (1984) 286.
- 2) Y. Sawada, A. Dougherty and J. P. Gollub: *Phys. Rev. Lett.* **56** (1986) 1260.
- 3) D. Grier, E. Ben-Jacob, R. Clarke and L. M. Sander: *Phys. Rev. Lett.* **56** (1986) 1264.
- 4) J. R. Melrose, D. B. Hibbert and R. C. Ball: *Phys. Rev. Lett.* **65** (1990) 3009.
- 5) P. P. Trigueros, J. Claret, F. Mas and F. Sagues: *J. Electroanal. Chem.* **312** (1991) 219.
- 6) M. Wang and N. Ming: *Phys. Rev. Lett.* **71** (1993) 113.
- 7) D. Barkey, F. Oberholtzer and Q. Wu: *Phys. Rev. Lett.* **75** (1995) 2980.
- 8) V. Fleury: *Nature* **390** (1997) 145.
- 9) J. A. Switzer *et al.*: *J. Mater. Res.* **13** (1998) 909.
- 10) M. Wang *et al.*: *Phys. Rev. Lett.* **86** (2001) 3827.
- 11) R. M. Suter and P. Wong: *Phys. Rev. B* **39** (1989) 4536.
- 12) C. Cachet, B. Saidani and R. Wiart: *J. Electrochem. Soc.* **138** (1991) 678.
- 13) C. Cachet, B. Saidani and R. Wiart: *J. Electrochem. Soc.* **139** (1992) 644.
- 14) M. Wang and N. Ming: *Phys. Rev. A* **45** (1992) 2493.
- 15) F. Argoul and A. Kuhn: *J. Electroanal. Chem.* **359** (1993) 81.
- 16) M. T. M. Koper: *J. Electroanal. Chem.* **409** (1996) 175.
- 17) M. T. M. Koper: *J. Chem. Soc., Faraday Trans.* **94** (1998) 1369.
- 18) P. Strasser, M. Eiswirth and M. T. M. Koper: *J. Electroanal. Chem.* **478** (1999) 50.
- 19) V. Fleury, J.-N. Chazalviel and M. Rosso: *Phys. Rev. Lett.* **68** (1992) 2492.
- 20) V. Fleury, J. H. Kaufman and D. B. Hibbert: *Nature* **367** (1994) 435.
- 21) M. Wang, W. J. P. van Enckevort, N. Ming and P. Bennema: *Nature* **367** (1994) 438.
- 22) K. Q. Zhang *et al.*: *Phys. Rev. E* **61** (2000) 5512.
- 23) F. Argoul and A. Arneodo: *J. Phys. (Paris)* **51** (1990) 2477.